

# A deletion in *FLS2* and its expansion after domestication caused global dissemination of melon cultivars defective in flagellin recognition

Chujia Jin<sup>1</sup>, Hiroki Matsuo<sup>1</sup>, Yoshizo Nakayama<sup>1</sup>, Gentaro Shigita<sup>2,3</sup>, Yoshihiro Inoue<sup>4</sup>, Kenji Kato<sup>5</sup> and Yoshitaka Takano<sup>1,\*</sup> 

<sup>1</sup>Laboratory of Plant Pathology, Graduate School of Agriculture, Kyoto University, Kyoto 606-8502 Japan,

<sup>2</sup>Laboratory of Plant Biodiversity Research, Department of Life Science Systems, Technical University of Munich, Freising 85354 Germany,

<sup>3</sup>Faculty of Life and Environmental Sciences, University of Tsukuba, Ibaraki 305-8572 Japan,

<sup>4</sup>Laboratory of Plant Genetics, Graduate School of Agriculture, Kyoto University, Kyoto 606-8502 Japan, and

<sup>5</sup>Graduate School of Environmental, Life, Natural Science and Technology, Okayama University, 1-1-1 Tsushima Naka, Kita-ku, Okayama 700-8530 Japan

Received 11 January 2024; revised 30 April 2024; accepted 13 June 2024; published online 26 June 2024.

\*For correspondence (e-mail [takano.yoshitaka.2x@kyoto-u.ac.jp](mailto:takano.yoshitaka.2x@kyoto-u.ac.jp))

## SUMMARY

**FLAGELLIN SENSING 2 (*FLS2*)** encodes a pattern recognition receptor that perceives bacterial flagellin. While putative *FLS2* orthologs are broadly conserved in plants, their functional characterization remains limited. Here, we report the identification of orthologs in cucumber (*Cucumis sativus*) and melon (*C. melo*), named *CsFLS2* and *CmFLS2*, respectively. Homology searching identified *CsFLS2*, and virus-induced gene silencing (VIGS) demonstrated that *CsFLS2* is required for flg22-triggered ROS generation. Interestingly, genome re-sequencing of melon cv. Lennon and subsequent genomic PCR revealed that Lennon has two *CmFLS2* haplotypes, haplotype I encoding full-length *CmFLS2* and haplotype II encoding a truncated form. We show that VIGS-mediated knockdown of *CmFLS2* haplotype I resulted in a significant reduction in both flg22-triggered ROS generation and immunity to a bacterial pathogen in melon cv. Lennon. Remarkably, genomic PCR of *CmFLS2* revealed that 68% of tested commercial melon cultivars possess only *CmFLS2* haplotype II: these cultivars thus lack functional *CmFLS2*. To explore evolutionary aspects of *CmFLS2* haplotype II occurrence, we genotyped the *CmFLS2* locus in 142 melon accessions by genomic PCR and analyzed 437 released sequences. The results suggest that *CmFLS2* haplotype II is derived from *C. melo* subsp. *melo*. Furthermore, we suggest that the proportion of *CmFLS2* haplotype II increased among the improved *melo* group compared with the primitive *melo* group. Collectively, these findings suggest that the deleted *FLS2* locus generated in the primitive *melo* subspecies expanded after domestication, resulting in the spread of commercial melon cultivars defective in flagellin recognition, which is critical for bacterial immunity.

**Keywords:** melon, *FLS2*, deletion, domestication, bacterial immunity.

**Linked article:** This paper is the subject of a Research Highlight article. To view this Research Highlight article visit <https://doi.org/10.1111/tpj.16957>.

## INTRODUCTION

To combat infections and colonization by phytopathogens, plants generally employ a two-layered surveillance system to activate their immune responses. As the first step in pathogen perception, plants recruit pattern recognition receptors (PRRs), located mainly at the cell surface, to recognize conserved features of pathogen-associated molecular patterns (PAMPs) and therefore initiate so-called PAMP-triggered immunity (PTI) (Monaghan & Zipfel, 2012).

To detect further invasion of pathogens that are capable of suppressing PTI successfully, plants have evolved a second layer of intracellular immune receptors to directly or indirectly recognize pathogen-secreted effector proteins and activate effector-triggered immunity (ETI) (Yuan et al., 2021). The initial perception of microorganisms mediated by PRRs is a fundamental process in plant immunity that plays a crucial role in defending plants against both adapted and non-adapted pathogens (Macho & Zipfel, 2014). Plant

PRRs are mainly comprised receptor-like kinases (RLKs) and receptor-like proteins (RLPs) (Boutrot & Zipfel, 2017; Couto & Zipfel, 2016). RLKs generally contain a leucine-rich repeat (LRR) ectodomain for ligand binding, a single-pass transmembrane (TM) domain, and an intracellular kinase domain, while RLPs usually lack the intracellular kinase domain (Saijo et al., 2018). The first characterized plant PRR was the RLK-type PRR FLAGELLIN-SENSITIVE2 (FLS2) in *Arabidopsis thaliana*, which is capable of perceiving a bacterial flagellin fragment called flg22 (Gómez-Gómez & Boller, 2000). Recognition of flg22 by FLS2 triggers multiple PTI responses including rapid reactive oxygen species (ROS) production (Wu et al., 2022). Importantly, loss-of-function *Arabidopsis* mutants for *FLS2* are more susceptible to the bacterium *Pseudomonas syringae* pv. *tomato* DC3000 (Zipfel et al., 2004). Moreover, the silencing of *FLS2* in tobacco and soybean led to enhanced susceptibility to *P. syringae* strains (Hann & Rathjen, 2007; Tian et al., 2020). All these findings demonstrate the importance of FLS2 in plant resistance against bacterial pathogens. Although the majority of plants possess *FLS2*-like sequences in their genomes (Cheng et al., 2020), loss-of-function analysis such as gene silencing and CRISPR-cas9 gene editing has so far been reported for only very limited *FLS2* orthologs as mentioned (Hann & Rathjen, 2007; Roberts et al., 2020; Tian et al., 2020; Wu et al., 2022; Zipfel et al., 2004). Especially, the examination of *FLS2* ortholog in cucumber performed by Wu et al. (2022) using transient expression assay in *FLS2*-knockout *Nicotiana benthamiana* suggested its possible insensitivity to several kinds of flg22. Thus, it remains unclear whether cucurbit plants possess functional FLS2 orthologs.

The plant family Cucurbitaceae (cucurbits) comprises 96 genera and approximately 1000 species including commercially important crops such as cucumber (*Cucumis sativus*), melon (*C. melo*), squash/pumpkin (*Cucurbita* spp.), and watermelon (*Citrullus lanatus*) (Endl et al., 2018; Renner & Schaefer, 2016; Rolnik & Olas, 2020). Cucurbit crops are cultivated worldwide and are mainly valued for their fruits and seeds, which provide numerous nutrients including carbohydrates, proteins, fats, and micronutrients for the human diet (Ogunbanjo et al., 2016). Yield and quality of cucurbit crops are seriously threatened by phytopathogenic bacteria (Akköprü et al., 2021; Burdman & Walcott, 2012). In particular, angular leaf spot disease caused by *P. syringae* pv. *lachrymans* (*Psl*) is prevalent among cucurbit crops throughout the world and may, for example, cause 30–60% reduction in cucumber production (Akköprü et al., 2021; Chai et al., 2020; Khlaif, 1995; Pohronezny et al., 1978). The symptoms of *Psl* infection start with the appearance of small, circular leaf spots; these later develop into water-soaked, vein-limited, irregular necrotic lesions on plant leaves or fruits, which can eventually result in foliar blight or fruit deformity (Olczak-Woltman et al., 2006, 2008).

In this study, we report the identification and functional characterization of FLS2 in cucumber and melon. ROS generation was detected in both cucumber (cv. Suyo) and melon (cv. Lennon) upon treatment with the commonly used *P. aeruginosa* flg22 peptide, suggesting the presence in both cucurbit cultivars of a flagellin receptor that can recognize flg22. The ortholog in cucumber, named CsFLS2, was identified through a homology search, and its function was then demonstrated by virus-induced gene silencing (VIGS) assay, that is, flg22-induced ROS generation was attenuated in *FLS2*-silenced cucumber (cv. Suyo) compared with non-silenced plants. In contrast, we found no clear *FLS2* homolog in the genome database of melon (cv. DHL92) released at that time, even though, as mentioned above, we detected flg22-induced ROS generation in melon cv. Lennon. We therefore sequenced the genome of melon cv. Lennon. Remarkably, mapping of the Lennon genome data and subsequent analyses revealed that this cultivar has two *FLS2* haplotypes, named *CmFLS2* haplotypes I and II. *CmFLS2* haplotype II lacks a major region of FLS2 and is presumed to be nonfunctional, while *CmFLS2* haplotype I encodes a full-length polypeptide. We also revealed the functionality of *CmFLS2* haplotype I by the VIGS assay. Surprisingly, we discovered that many commercial melon cultivars lack *CmFLS2* haplotype I and therefore cannot elicit ROS generation upon flg22 treatment. Furthermore, haplotype I-silenced melon cultivar plants displayed reduced immunity to *Psl* compared with non-silenced plants, strongly suggesting that the deletion in *FLS2* has a negative impact on immunity traits of commercial melon cultivars.

We then investigated the evolutionary aspects of this mutation by analyzing 142 melon accessions. This revealed that the deletion in *FLS2* occurred in a primitive landrace of *C. melo* subsp. *melo* and has become prevalent in improved accessions of this subspecies, including modern Japanese commercial cultivars. These results provide compelling evidence that human domestication and subsequent selection have unexpectedly led to a negative impact on melon disease resistance, although we can now prevent this by the application of a molecular marker for *FLS2* in breeding.

## RESULTS

### Oxidative burst detection in cucurbits upon flg22 treatment and identification of cucumber functional FLS2

Homologs of *FLS2* are thought to be conserved in most higher plants (Wu et al., 2022). To determine whether cucurbit crops harbor a functional FLS2 that can perceive the bacterial flagellin epitope flg22 and therefore trigger plant immunity, we monitored the oxidative burst induced by flg22 as a defense marker event in cucumber (cv. Suyo) and melon (cv. Lennon). After treatment with 1  $\mu$ M flg22, leaf discs of both Suyo and Lennon displayed a transient and rapid ROS burst (Figure 1a). Maximal ROS production

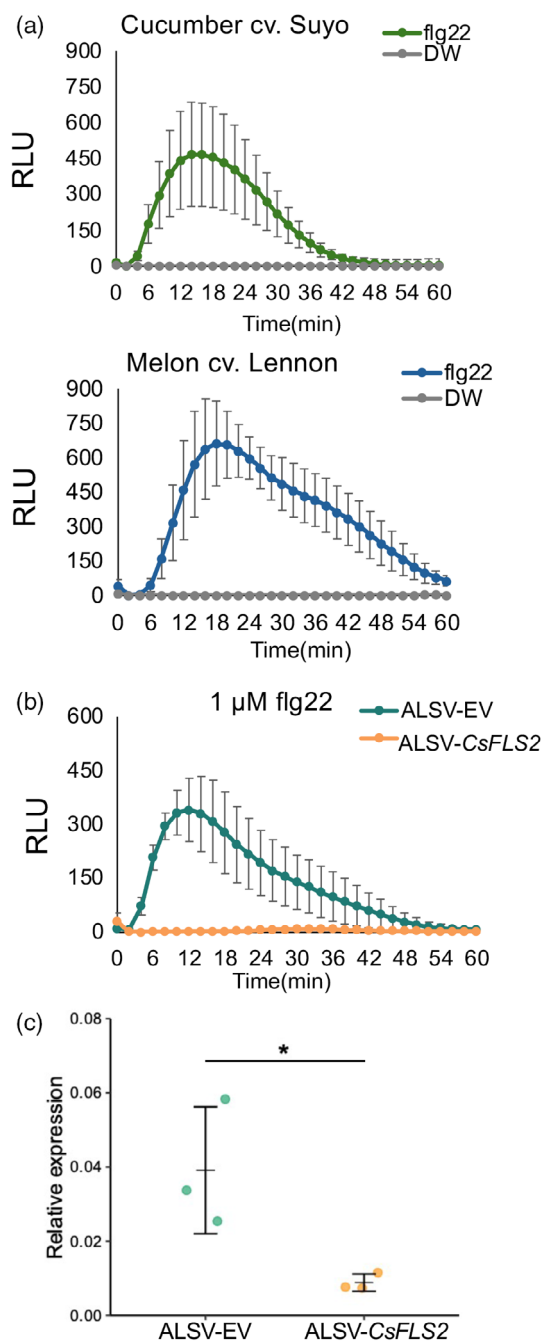


**Figure 1.** flg22-triggered ROS production in cucurbits and functional validation of cucumber FLS2 receptor.

(a) ROS burst was measured for 60 min in cucumber cv. Suvo (upper) and melon cv. Lennon (lower) leaf discs after treatment with 1 μM flg22 or distilled water (DW). The data were collected from three plants for each treatment ( $n = 3$ ). Values are mean  $\pm$  SD. Total ROS production is represented as relative luminescence units (RLU). Similar results were obtained from two additional experiments.

(b) ROS burst detection for 60 min using cucumber cv. Suvo leaf discs collected from the fourth true leaf (counting from bottom to top) of ALSV-EV or ALSV-CsFLS2 infected plants following treatment with 1 μM flg22. The data were collected from three plants for each treatment ( $n = 3$ ). Values are mean  $\pm$  SD. Total ROS production is represented as RLU. Similar results were obtained from two additional experiments.

(c) RT-qPCR analysis showing the expression of *CsFLS2* transcripts in the fourth true leaf (counting from bottom to top) of ALSV-EV or ALSV-CsFLS2 infected cucumber cv. Suvo, using primers specific for *CsFLS2*. Cucurbit *Actin* was used as the internal control in the reaction for normalization of gene expression level. The data were collected from three plants for each treatment ( $n = 3$ ). Data represent the mean  $\pm$  SD. \* $P < 0.05$ . Similar results were obtained from two additional experiments.

cucumber displayed less than 39% identity. We named the candidate *CsFLS2*. Its amino acid (aa) sequence also showed identities of 57% with *Nicotiana benthamiana* NbFLS2, 48% with rice OsFLS2, 57% with tomato SIFLS2, and 62% with grapevine VvFLS2 (Figure S1). The putative *CsFLS2* gene (*CsaV3\_6G051540*) has a 3471-bp open reading frame that encodes a 1156-aa protein and contains one short 269-bp intron at position 3131, a structure that is also similar to the *AtFLS2*, *SIFLS2*, *OsFLS2*, and *VvFLS2* genes (Trdá et al., 2014). The deduced *CsFLS2* protein contains a signal peptide, an extracellular LRR domain, a TM domain, and a serine/threonine kinase domain (Figure S2). Consistent with *AtFLS2*, *SIFLS2*, and *VvFLS2*, *CsFLS2* contains 28 tandem repeats in its LRR domain. These findings suggest that *CsFLS2* is a strong candidate for the functional ortholog of FLS2 in cucumber.

To obtain further evidence for this, we carried out a virus-induced gene silencing (VIGS) assay of *CsFLS2* in cucumber (cv. Suvo) using an *apple latent spherical virus* (ALSV) vector (Igarashi et al., 2009; Kawai et al., 2014). We first tested the efficiency of the *Agrobacterium* infiltration-based VIGS system in cucumber by silencing the *PDS* (*phytoene desaturase*) gene of cucumber, which we can evaluate by detecting its bleached phenotype (Igarashi et al., 2009). The third true leaf (counting from bottom to top) of ALSV-*CsPDS*-infiltrated cucumber started to turn white at 16–19 days after infiltration. A highly uniform white photobleached phenotype then appeared on the fourth true leaf (Figure S3). A similar result was obtained for the silencing of the melon *PDS* gene (*CmPDS*) using the same method (Figure S3), indicating that this *Agro*-infiltration-based VIGS system is a feasible way to validate gene function in both cucumber and melon. Therefore, to silence *CsFLS2* in cucumber (cv. Suvo), a 300-nucleotide fragment located in the LRR domain of *CsFLS2* was selected for *FLS2* silencing in Suvo. Compared to ALSV

in Suvo was detected at 14 min after flg22 treatment, while ROS production in Lennon peaked at 18 min. The finding that flg22 treatment can trigger ROS production in Suvo and Lennon strongly suggests the existence of functional FLS2 in both cucurbit cultivars.

We first attempted to identify the corresponding flagellin receptor in cucumber using BLASTP to search for an ortholog of *AtFLS2*. The search identified one strong candidate whose protein sequence exhibited 53% identity with *AtFLS2*, while other LRR receptor-like kinase proteins in

empty vector (ALSV-EV)-infiltrated cucumber, no growth defect was observed in ALSV-*CsFLS2*-infiltrated plants (Figure S4). We then tested flg22-triggered ROS generation in *CsFLS2*-silenced plants and control plants. ROS production in *CsFLS2*-silenced plants was almost abolished but was clearly detected in the control plants (Figure 1b). We also confirmed that the transcript level of *CsFLS2* was significantly reduced in the silenced plants in comparison with empty vector control plants (Figure 1c). These results demonstrate that *CsFLS2* is a functional ortholog of *AtFLS2* and is essential for flg22 perception in cucumber.

### Two *FLS2* haplotypes exist in the melon cultivar Lennon

We next searched for an *FLS2* ortholog in melon using the sequence of *CsFLS2*. Unexpectedly, a BLASTP search against the melon (cv. DHL92) reference database (DHL92 v3.6.1) detected only a gene named MELO3C007152.2, which likely contains (i) a deleted *FLS2*-homologous sequence, lacking most of the LRR, TM, and kinase domains, in the N terminal region of the predicted protein and (ii) a sequence unrelated to *FLS2* in the downstream region. Therefore, we re-sequenced melon cv. Lennon, which was shown to respond to flg22 (Figure 1a). As expected from the fact that Lennon is an F<sub>1</sub> hybrid cultivar, the average allele

frequencies in SNP sites were around 0.5, indicating that Lennon has a heterozygous genotype in the *FLS2* locus of the DHL92 reference genome (Figure 2a). By further examining Lennon sequence read alignments to this region, we observed a local drop of sequence depth coverage (Figure 2a) and elevated unpaired reads density (Figure 2a) within the putative pseudogenized *FLS2* sequence region (at chr08:1143516), suggesting a sequence insertion in one of the haplotypes of Lennon.

To investigate the *FLS2* sequence region in Lennon, we performed genomic PCR using Lennon genomic DNA as a template and detected two PCR amplicons (Figure 2b), which were subjected to Sanger sequencing. The longer amplicon of 3736 bp contained a full-length *FLS2* sequence showing ~96% amino acid sequence identity with *CsFLS2*, and we designated this as *CmFLS2* haplotype I (Figure 2c; Figures S5 and S6). On the other hand, the shorter amplicon of 759 bp had a sequence identical to the pseudogenized *FLS2* sequence in the DHL92 reference genome, and we designated this as *CmFLS2* haplotype II (Figure 2c; Figure S6). We conclude that melon cv. Lennon has a heterozygous genotype at the *FLS2* locus; haplotype I encodes full-length *FLS2* and haplotype II encodes a pseudogenized *FLS2* lacking most of the functional domains.

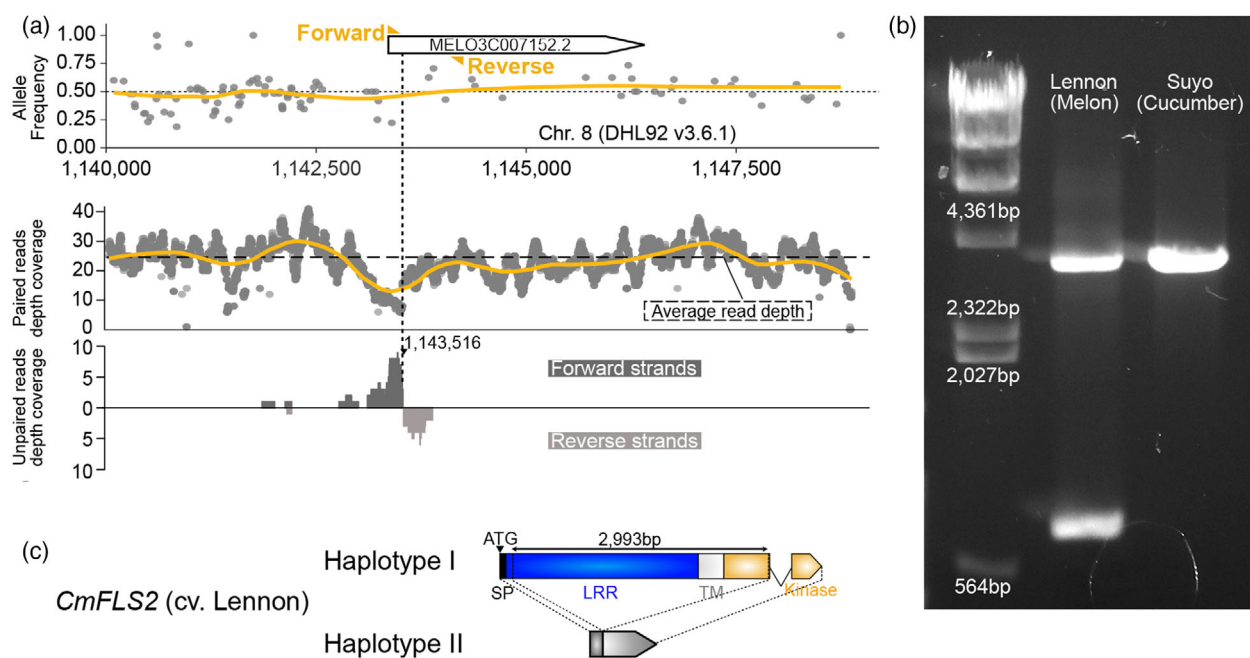


**Figure 2.** *In silico* identification of commercial F<sub>1</sub> hybrid cultivar “Lennon” *FLS2* locus and PCR amplification of cucurbit *FLS2*s.

(a) Allele frequency (top), paired reads (middle), and unpaired reads (bottom) depth coverage of Lennon against the *FLS2* locus in the reference genome DHL92 (v 3.6.1). Sequence reads of Lennon were aligned against the *FLS2* locus in DHL92. The average read depth is shown as dashed lines. Yellow lines correspond to the approximate curve of allele frequency (top) and the approximate curve of paired reads depth coverage (middle), respectively. Positions of forward and reverse primers used for subsequent genomic PCR are also shown.

(b) Amplification of *CmFLS2* and *CsFLS2* in melon (Lennon) and cucumber (Suyo). Genomic PCR was performed using the *CsCmFLS2\_check* primer pair.

(c) Schematic diagram of the exon–intron architecture of *CmFLS2* haplotype I and haplotype II. Colored boxes represent exon-encoded domains, and the folded line represents an intron.

Since the inferred CmFLS2 sequence in haplotype I shares a similar domain constitution with other FLS2 orthologs (Figure S5), we tested whether this gene is responsible for Lennon's ability to respond to flg22. To silence the CmFLS2 gene in haplotype I, an ALSV-based silencing vector carrying a 300-bp fragment specific to haplotype I (ALSV-CmFLS2-I) was constructed and introduced into Lennon. ROS production upon flg22 treatment was diminished in ALSV-CmFLS2-I-infiltrated plants, but they showed no growth defect in comparison with empty vector control (ALSV-EV) plants (Figure 3a,b). We also confirmed that CmFLS2 expression decreased significantly in the ALSV-CmFLS2-I-infiltrated plants (Figure 3c). These results indicate that CmFLS2 haplotype I, but not CmFLS2 haplotype II, encodes a functional FLS2 receptor in commercial melon cultivar Lennon to sense flg22.

### The CmFLS2 genotype varies among commercial melon cultivars and correlates with sensitivity to flg22

As described above, the melon commercial cultivar Lennon possesses two haplotypes of CmFLS2, while the cultivar DHL92 likely possesses only CmFLS2 haplotype II and lacks the haplotype I, based on BLASTP analysis against the genome annotation data. These findings raise the possibility that the FLS2 genotype differs among cucurbit cultivars, especially melon cultivars. Based on the identified CsFLS2 genome sequence data, we designed a pair of primers to amplify the CsFLS2 gene from the cucumber cultivar Suvo, which are the same as the primers used for amplifying CmFLS2. Only one band of approximately 3.7 kb was amplified, and subsequent Sanger sequencing of the product confirmed that it is CsFLS2. Taking advantage of this primer pair, we attempted to genotype the FLS2 locus in different cucumber and melon cultivars via genome PCR. Twelve additional commercial melon cultivars and eight additional commercial cucumber cultivars were investigated. All eight commercial cucumber cultivars showed a single band after PCR amplification, whose size was identical to that of the product from Suvo. This finding indicates that all tested commercial cucumber cultivars only possess full-length CsFLS2 (Figure 4a).

To test the possibility that cucumber cultivars have a CsFLS2 deletion or null allele (given that we would detect no products in the PCR-based genotyping), in addition to the full-length CsFLS2 allele, we mapped the sequence reads of Suvo to the genome of different cucumber accessions. Analysis of the mapping results around CsFLS2 revealed high and averaged read depth coverage, as well as low unpaired read density in this area (Figure S7). Furthermore, we investigated the CsFLS2 genotype of F<sub>1</sub> and F<sub>2</sub> progenies of two cucumber accessions and found that all tested F<sub>2</sub> progeny showed only one band with the same size as their parents (Figure S8a). All results supported the

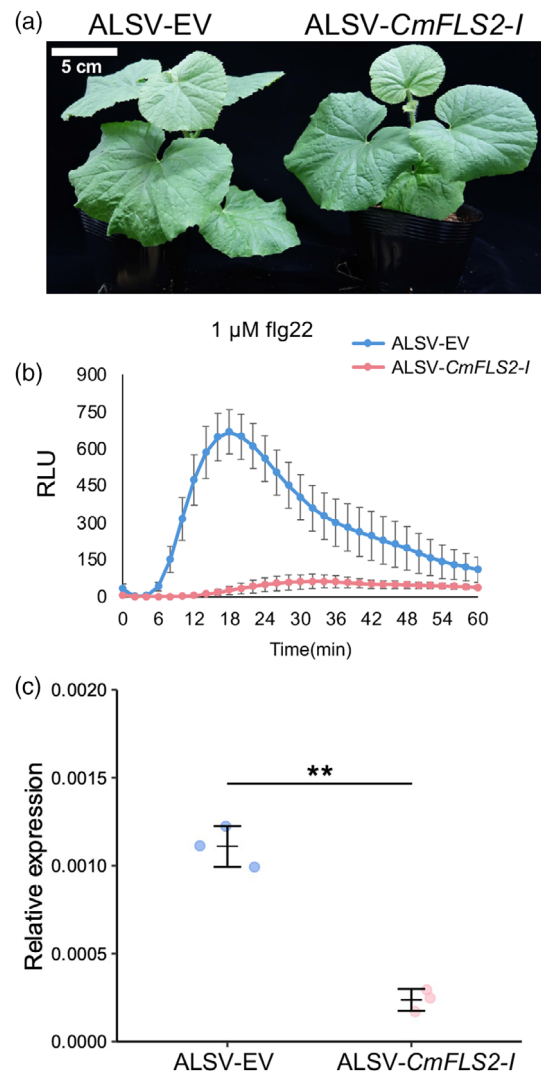


**Figure 3.** Functional validation of melon FLS2 haplotype I.

(a) Plant growth comparison between melon cv. Lennon infected with ALSV-EV (left) and ALSV-CmFLS2-I (right). The photo was taken at 35 days post-infiltration. Similar results were obtained from two additional experiments.

(b) ROS burst detection for 60 min using melon cv. Lennon leaf discs collected from the fourth true leaf (counting from bottom to top) of ALSV-EV or ALSV-CmFLS2-I-infected plants following treatment with 1  $\mu$ M flg22. The data were collected from three plants for each treatment ( $n = 3$ ). Values are mean  $\pm$  SD. ROS production is represented as RLU. Similar results were obtained from two additional experiments.

(c) RT-qPCR analysis showing the expression of CmFLS2 haplotype I transcripts in the fourth true leaf (counting from bottom to top) of ALSV-EV or ALSV-CmFLS2-I-infected melon cv. Lennon, using primers specific for CmFLS2 haplotype I. Melon *Actin* was used as the internal control in the reaction for normalization of gene expression level. The data were collected from three plants for each treatment ( $n = 3$ ). Data represent the mean  $\pm$  SD. \*\* $P < 0.01$ . Similar results were obtained from two additional experiments.

idea that full-length CsFLS2 is homozygous in all tested cucumber cultivars.

Interestingly, CmFLS2 genotype varied among the tested melon cultivars (Figure 4a). Two melon cultivars

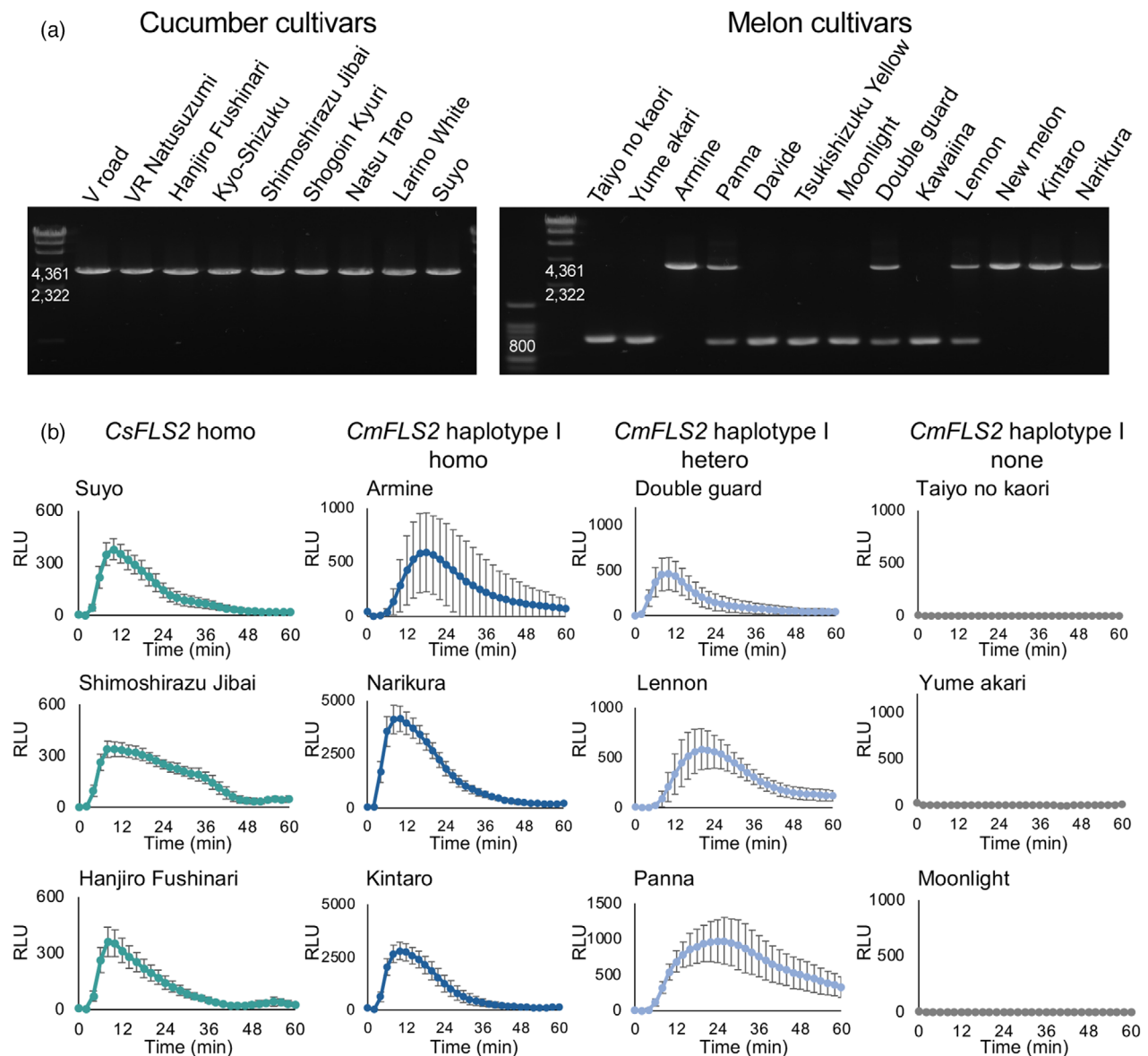


**Figure 4.** Genotyping of *FLS2* and flg22 sensitivity in commercial cucumber and melon cultivars.

(a) Genotyping of the *FLS2* locus in commercial cucumber and melon cultivars. Ten- to 14-day-old plants were used for genotyping. Genomic PCR was performed using a *CsCmFLS2\_check* primer pair. Genomic PCR in cucumber cultivars only detected full-length *CsFLS2* (*CsFLS2* homo). Genomic PCR in melon cultivars revealed three types: cultivars showing only the full-length *FLS2* band (*CmFLS2* haplotype I homo), cultivars showing both full-length and short *FLS2* bands (*CmFLS2* haplotype I hetero), and cultivars showing only the short *FLS2* band (*CmFLS2* haplotype I none).

(b) flg22-triggered ROS burst assay in commercial cucumber and melon cultivars. The ROS burst was measured for 60 min using leaf discs of the different cultivars after treatment with 1  $\mu$ M flg22. The data were collected from 12 individual leaf disks from a single plant of each cultivar ( $n = 12$ ). Values are mean  $\pm$  SD. ROS production is represented as RLU. Similar results were obtained from two additional experiments.

(Panna and Double guard) had the same two bands as Lennon and were classified as *CmFLS2* haplotype I heterozygous type. Six melon cultivars showed only one short band with the same size as *CmFLS2* haplotype II; we named them *CmFLS2* haplotype I none type. Four melon cultivars showed only one long band with the same size as *CmFLS2* haplotype I, indicating that they only possess *CmFLS2* haplotype I, encoding functional full-length *CmFLS2*. Moreover, all tested  $F_2$  progeny derived from a cross of two melon

cultivars that only showed *CmFLS2* haplotype I also displayed *CmFLS2* haplotype I (Figure S8b), and no progeny showed a possible *CmFLS2* deletion or null allele lacking any PCR products. Therefore, we categorized this genotype as *CmFLS2* haplotype I homozygous type.

We next investigated the relationship between *FLS2* genotypes and flg22 perception using flg22-treated ROS burst assays. Upon 1  $\mu$ M flg22 treatment, leaf discs from all tested commercial cucumber cultivars generated ROS,

which was consistent with their *CsFLS2* full-length homozygous genotype (Figure 4b). Leaf discs from *CmFLS2* haplotype I homozygous and heterozygous melon cultivars were able to respond to flg22 (Figure 4b). In contrast, there was no ROS production upon flg22 treatment in any of the melon cultivars lacking *CmFLS2* haplotype I (Figure 4b), although these cultivars were still able to respond to the unrelated fungal PAMP chitin (Figure S9), demonstrating the occurrence of loss of flg22-sensing ability in these cultivars. Taken together, these results indicate that the *CmFLS2* genotype varies among commercial melon cultivars and that the presence/absence polymorphism of the *CmFLS2* haplotype I, that is, functional *CmFLS2*, is correlated with their flg22 perception ability.

### **CmFLS2 is involved in immunity against *Pseudomonas syringae* pv. *lachrymans* in melon**

Loss-of-function analysis of putative *FLS2* orthologs showed that FLS2 is involved in immunity against bacterial pathogens in *Arabidopsis*, tomato, tobacco, and soybean (Hann & Rathjen, 2007; Roberts et al., 2020; Tian et al., 2020; Zipfel et al., 2004). Since FLS2-mediated flg22 perception was lost in some melon cultivars, we asked whether functional *CmFLS2* (haplotype I) in melon is involved in basal resistance against bacterial pathogens. *Pseudomonas syringae* pv. *lachrymans* (*Psl*) is known to cause angular leaf spots on cucurbit plants such as cucumber, watermelon, and melon (Newberry et al., 2016). Because the melon cultivar Lennon has a functional *CmFLS2* haplotype, we performed a *Psl* inoculation assay on *CmFLS2* haplotype I-silenced Lennon. We first checked ROS production triggered by flg22 derived specifically from the *Psl* strain (flg22<sup>Psl</sup>) that we later used in the inoculation experiment. Compared with empty vector-infiltrated Lennon, flg22<sup>Psl</sup>-triggered ROS production was almost abolished in the *CmFLS2* haplotype I-silenced Lennon (Figure 5a), indicating that sensitivity to flg22<sup>Psl</sup> was severely impaired when *CmFLS2* haplotype I was silenced; in other words, *CmFLS2* senses the flg22 epitope of *Psl* flagellin. We then tested whether this defect affects Lennon's immunity to *Psl*. The fourth leaves of tested plants were sprayed with *Psl* suspension. At 4 days post-inoculation (dpi), the leaves of *CmFLS2* haplotype I-silenced plants showed more severe symptoms than those of empty vector control plants (Figure 5b). We also measured bacterial growth by a DNA-based real-time PCR assay (Ross & Somssich, 2016). Consistent with the disease symptoms, *Psl* growth was significantly higher in the *CmFLS2*-silenced Lennon plants than in the empty vector control (*CmFLS2*-non-silenced) plants (Figure 5c). These results strongly suggest that full-length *CmFLS2*, which is essential for flg22-triggered ROS generation, is involved in immunity against the bacterial pathogen in the melon commercial cultivar Lennon.

We next examined the impact of the natural deficiency of functional *CmFLS2* on melon immunity against *Psl*. Two melon cultivars, Harukei-3 and EDISTO 47 (INRA), exhibiting a close phylogenetic relationship (Shigita et al., 2023) but displaying a distinct *CmFLS2* genotype (Table S1), were selected and inoculated with *Psl*. As anticipated, the leaves of Harukei-3 (*CmFLS2* haplotype I none) plants displayed more severe symptoms than EDISTO 47 (INRA) (*CmFLS2* haplotype I homozygous) plants at 4 dpi (Figure 5d). DNA-based measurements of bacterial growth on plant leaves confirmed that the *CmFLS2* haplotype I-lacking cultivar Harukei-3 is more susceptible to *Psl* than the *CmFLS2* haplotype I homozygous cultivar EDISTO 47 (INRA) (Figure 5e), providing further compelling evidence that *CmFLS2* is critical for melon immunity against bacterial infection.

### **Evolutionary aspects of *CmFLS2* haplotype occurrence in melon**

Although our *Psl* inoculation assay revealed the importance of *CmFLS2* for immunity against a bacterial pathogen in melon, we also found that particular commercial melon cultivars have lost the functional *CmFLS2* gene (haplotype I). To gain further insights into the occurrence of loss of functional *CmFLS2*, we performed PCR-based genotyping of the *CmFLS2* locus using genome DNAs of 142 melon accessions from the Japanese National Agriculture and Food Research Organization (NARO) Genebank and an additional 15 commercial F<sub>1</sub> hybrid cultivars from different seed companies in Japan (Table S2).

Melon has been divided into two subspecies, *C. melo* L. subsp. *agrestis* (hereafter *agrestis*) and *C. melo* L. subsp. *melo* (hereafter *melo*), based on hair features on their ovaries (Kirkbride, 1993). Melon accessions can be classified based on their chloroplast genome or nuclear genome (Shigita et al., 2023). We here investigated cytoplasm types based on the chloroplast genome. Melon accessions from NARO Genebank used in our study were divided into three cytoplasm types (Ia, Ib, Ic) based on a previous report (Shigita et al., 2023; Figure 6a).

All nine accessions in the Ic-type group, which is exclusively distributed in Africa, only possess functional full-length *CmFLS2* haplotype I (Figure 6a,b). In the Ia-type group, *CmFLS2* haplotype I is also highly conserved: the occurrence of this haplotype is 91% (126/138) (Figure 6a,b; Table S1). Notably, 88% (61/69) accessions of the Ia-type group display *CmFLS2* haplotype I homozygous type. Surprisingly, we found that the ratio of *CmFLS2* haplotype II was much higher in the Ib-type group than in the other two groups. The occurrence of haplotype II is 70% (89/128) in the Ib-type group, and 66% (42/64) accessions are the *CmFLS2* haplotype I none type that lacks functional *CmFLS2* (Figure 6a,b; Table S1). Notably, Shigita et al. (2023) and Tanaka et al. (2013) reported an association

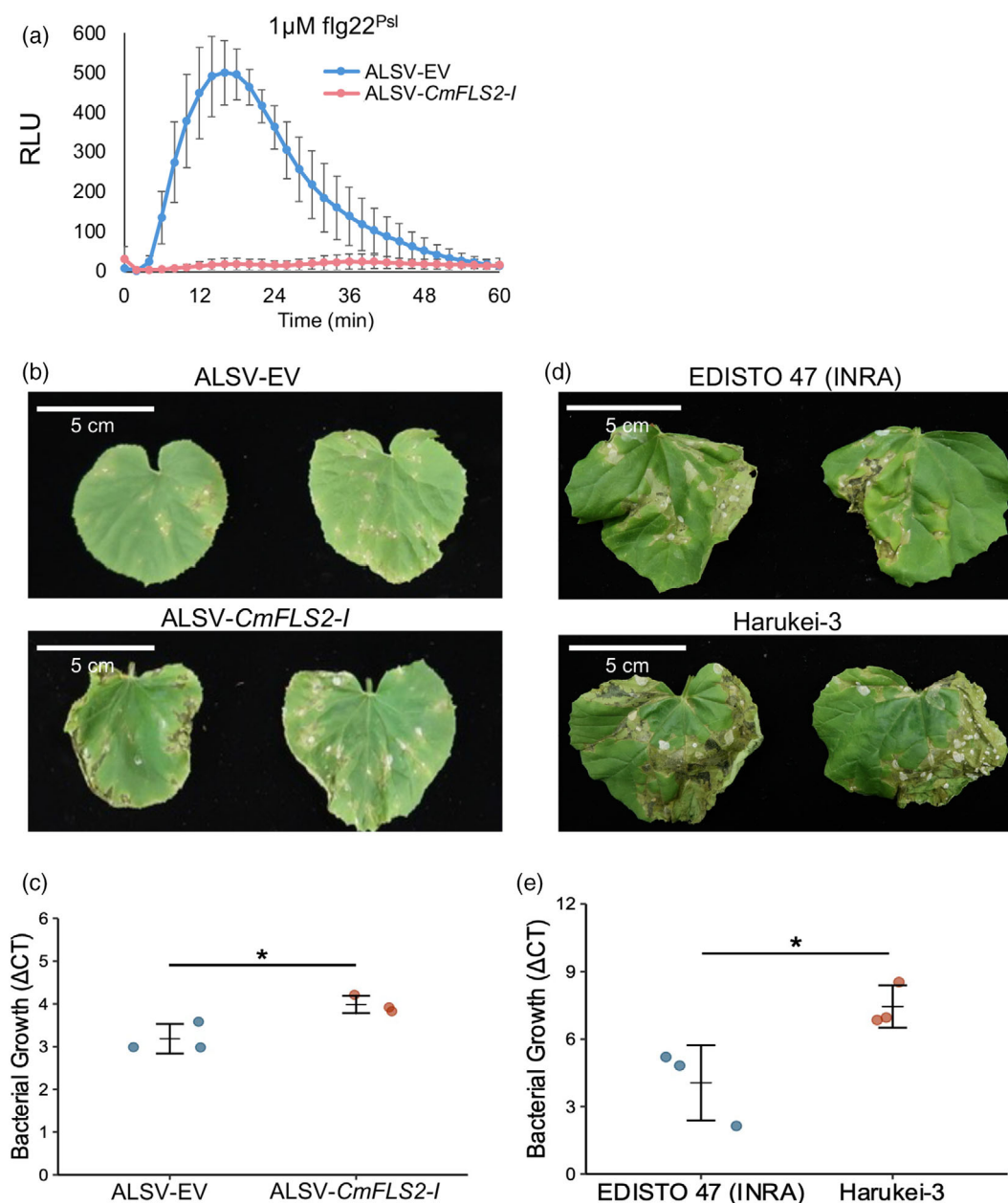


**Figure 5.** Involvement of CmFLS2 in melon resistance against *PsI*.

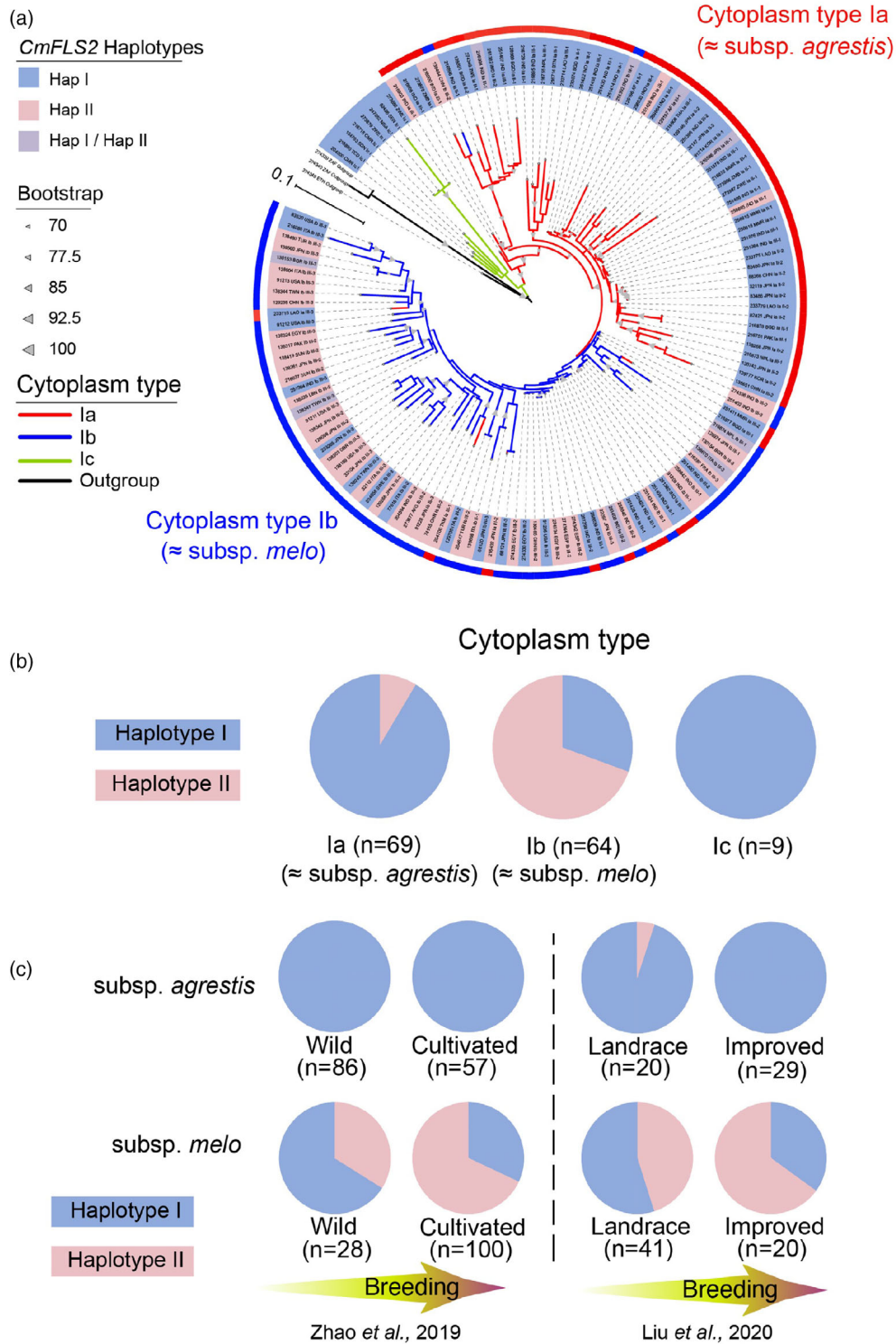
(a) ROS burst was measured for 60 min using melon cv. Lennon leaf discs infected with ALSV-EV or ALSV-CmFLS2-I after treatment with 1  $\mu\text{M}$  flg22<sup>Psl</sup>. The data were collected from three plants for each treatment ( $n = 3$ ). Values are mean  $\pm$  SD. Total ROS production is represented as RLU. Similar results were obtained from two additional experiments.

(b) Comparison of the symptoms caused by *PsI* on ALSV-EV-infected and ALSV-CmFLS2-I-infected Lennon leaves. Forty-day-old VIGS melon plants were spray-inoculated with *PsI*. Similar results were obtained from two additional experiments.

(c) Measurement of *PsI* growth on VIGS-treated Lennon. qPCR-based biomass validation was used to quantify *PsI* growth. The relative abundance of bacteria compared to plant cells was measured by subtracting the bacterial *oprF* gene Ct value from the melon *Actin* gene Ct value ( $\Delta\text{CT}$ ). The data were collected from three plants for each treatment ( $n = 3$ ). Data represent the mean  $\pm$  SD.  $*P < 0.05$ . Similar results were obtained from two additional experiments.

(d) Comparison of the symptoms caused by *PsI* on closely related melon cultivars with a distinct *CmFLS2* genotype. Melon cultivar EDISTO 47 (INRA) is a *CmFLS2* haplotype I homozygous type, while Harukei-3 is a *CmFLS2* haplotype I none type. Twenty-day-old melon seedlings were spray-inoculated with *PsI*. Similar results were obtained from two additional experiments.

(e) Measurement of *PsI* growth on closely related melon cultivars with a distinct *CmFLS2* genotype. Melon cultivar EDISTO 47 (INRA) is a *CmFLS2* haplotype I homozygous type, while Harukei-3 is a *CmFLS2* haplotype I none type. Similar results were obtained from two additional experiments. The relative abundance of bacteria compared to plant cells was measured by subtracting the bacterial *oprF* gene Ct value from the melon *Actin* gene Ct value ( $\Delta\text{CT}$ ). The data were collected from three plants for each treatment ( $n = 3$ ). Data represent the mean  $\pm$  SD.  $*P < 0.05$ . Similar results were obtained from two additional experiments.



between cytoplasm types and melon subspecies, that is, la-type and lb-type accessions largely correspond to *agrestis* and *melo*, respectively. As for lc-type melon accessions, they formed a unique clade different from *agrestis* and *melo* (Shigita et al., 2023). Taken together, these results showed that functional *CmFLS2* haplotype I is strongly conserved among *agrestis* and the unique African groups, while the *CmFLS2* genotype is more diverse in *melo* and the occurrence of nonfunctional *CmFLS2* haplotype II was markedly increased in this subspecies.

We next took advantage of public sequence read archive (SRA) data derived from Liu et al. (2020) and Zhao et al. (2019) to investigate *in silico* the distribution of *CmFLS2* haplotypes in more melon accessions belonging to *agrestis* or *melo*. Zhao et al. (2019) further classified both *agrestis* and *melo* into two groups each, relatively primitive groups (labeled “wild”) and relatively improved groups (“cultivated”). Similarly, Liu et al. (2020) also categorized them into landrace and improved groups. All four *agrestis* groups mostly possessed the functional *CmFLS2* haplotype I only, whereas the *melo* groups comprised a mixture of both haplotypes (Figure 6c). Importantly, in *melo* accessions, we found that the proportion of nonfunctional *CmFLS2* haplotype II was higher in the “cultivated” group (69%) than in the “wild” group (34%) in the analysis of SRA data from Zhao et al. (2019) (Figure 6c; Table S3), possibly suggesting that nonfunctional *CmFLS2* haplotype II generated in a relatively primitive accession expanded to the relatively improved groups. Consistent with this idea, we found that the proportion of *CmFLS2* haplotype II was higher in the improved group (65%) compared to the landrace group (45%) in the analysis of SRA data from Liu et al. (2020) (Figure 6c; Table S3). We also investigated the proportion of *CmFLS2* haplotype II in commercial F<sub>1</sub> hybrid cultivars and found that it was 75% (42/56) (Figure S10). Collectively, these findings suggest that nonfunctional *CmFLS2* haplotype II originated in a primitive *melo* accession and subsequently expanded to improved *melo* accessions, including modern commercial cultivars.

## DISCUSSION

Flagellin, the main component of the bacterial flagellum, is indispensable for motility and is strongly associated with the infectivity of many pathogenic bacteria (Finlay & Falkow, 1997; Gómez-Gómez & Boller, 2002; Tans-Kersten et al., 2001). Therefore, it is unsurprising that many higher organisms including both animals and plants have acquired the ability to recognize flagellin as a PAMP to protect themselves from bacterial pathogens (Chinchilla et al., 2006; Felix et al., 1999). The flagellin perception receptor, designated FLS2, was first identified in *A. thaliana* (Gómez-Gómez & Boller, 2000; Zipfel et al., 2004) and functional orthologs were then found in tomato, rice, soybean, tobacco, grapevine, and citrus plants through BLAST searching and

subsequent functional analyses including *Agrobacterium*-mediated transient expression and the complementation assay of the *Arabidopsis fls2* mutant (Hann & Rathjen, 2007; Robatzek et al., 2007; Shi et al., 2016; Takai et al., 2008; Tian et al., 2020; Trdá et al., 2014).

Here, we identified functional FLS2 orthologs in cucumber and melon, which is the first report of FLS2 in cucurbit plants. By taking advantage of the identified cucumber FLS2 sequence, we searched for its homologs in more cucurbit species by BLASTP. Most of the searched cucurbit plants, that is, bitter melon, bottle melon, chayote, snake melon, sponge melon, watermelon, and wax melon, possess an *FLS2*-homologous gene in their genome (Figure S11). However, we failed to find homologs that share more than 40% identity with CsFLS2 in the available sequence data of plants belonging to the genus *Cucurbita*. More research is necessary to reveal whether *Cucurbita* spp. possess *FLS2*.

Notably, melon contains two *FLS2* haplotypes: *CmFLS2* haplotype II encodes a protein lacking most of the LRR, TM, and kinase domains, whereas *CmFLS2* haplotype I encodes a protein in which these domains are intact (Figures S5 and S6). VIGS assay revealed that CsFLS2 and *CmFLS2* haplotype I are functional orthologs of AtFLS2 in cucumber and melon, respectively.

Surprisingly, we found that many tested melon cultivars lacked *CmFLS2* haplotype I (intact and functional *FLS2*), even though *FLS2* has been shown to be important for bacterial immunity in several plants (Hann & Rathjen, 2007; Roberts et al., 2020; Tian et al., 2020; Zipfel et al., 2004). In contrast, we found that all tested commercial cucumber cultivars encode only full-length CsFLS2. We also revealed that the melon cultivars lacking *CmFLS2* haplotype I were unable to generate ROS upon flg22 treatment, further supporting the idea that *CmFLS2* haplotype I is a receptor that recognizes flg22 and that flg22 recognition in melon depends solely on *CmFLS2* haplotype I.

Importantly, an inoculation assay using the bacterial pathogen *Psi* revealed more severe symptoms and increased growth of *Psi* in *CmFLS2* haplotype I-silenced melon (cv. Lennon), indicating that *CmFLS2* haplotype I is required for antibacterial immunity. Consistent with this, we also found that melon cv. Lennon triggers ROS production upon treatment with not only *Psi* flg22 but also *P. aeruginosa* flg22 peptide. Furthermore, the *Psi* inoculation assay on both the *CmFLS2* haplotype I homozygous cultivar EDISTO 47 (INRA) and the *CmFLS2* haplotype I none cultivar Harukei3 also strongly suggested that the deletion in *CmFLS2* haplotype I significantly reduced the immunity to this bacterial pathogen. These findings clearly suggest that the loss of functional *FLS2* (*CmFLS2* haplotype I) has a negative impact on disease resistance in melon.

We further investigated evolutionary aspects of the loss of functional *FLS2* in melon. For the melon genome,

genetic diversity has been shown to be significantly decreased in elite cultivars, most likely as a result of selection during breeding (Sanseverino et al., 2015). As described above, melon accessions can be classified based on their chloroplast genome (Shigita et al., 2023). For cytoplasm types based on the chloroplast genome, melon accessions belonging to la-type and lb-type are suggested to mostly correspond to *agrestis* and *melo* subspecies, respectively (Tanaka et al., 2013).

PCR-based genotyping of the *CmFLS2* locus showed that a majority of tested la-type melon accessions only harbor full-length functional *CmFLS2* (*CmFLS2* haplotype I) (Figure 6a; Table S1). These results suggest that the *FLS2*-dependent flg22 perception mechanism is highly conserved in *agrestis*. This idea is further supported by our informatic analyses of the publicly available data, which showed that 191 of 192 genotyped *agrestis* accessions have only full-length *CmFLS2* (Table S3).

In contrast, our PCR-based genotyping revealed that the *CmFLS2*-deleted genotype is extremely common in lb-type accessions, which predominantly belong to *melo*. This finding strongly suggests that the truncated nonfunctional *CmFLS2* haplotype II is derived from the *melo* subspecies. Furthermore, our analyses of SRA data suggested that the nonfunctional *CmFLS2* haplotype II was more abundant in the “cultivated” (relatively improved) or improved *melo* accessions than in the “wild” (relatively primitive) or landrace *melo* accessions (Figure 6c).

Collectively, these results suggested that the proportion of nonfunctional *CmFLS2* haplotype II dramatically increased among the improved subsp. *melo* accessions in comparison with the primitive subsp. *melo* accessions. Moreover, a majority of current commercial melon cultivars harbor *CmFLS2* haplotype II (Figure S10). These findings suggest that human domestication likely accelerated the loss of functional *FLS2* in melon cultivars. Although modern melon cultivars possess diverse domestication traits, continuous selection for a limited number of desired traits has resulted in a significant reduction of genetic diversity in cultivated melons (Zhao et al., 2019). In other words, melon has undergone severe bottlenecks during domestication. The low genetic diversity in cultivated melons is also likely linked to the expansion of the *CmFLS2* haplotype II in current commercial melon cultivars.

It is counterintuitive that *CmFLS2* haplotype II is predominant in improved *melo* accessions, given that it increases susceptibility to bacterial diseases and appears to be disadvantageous for melon. Two hypotheses could explain this enigma. The first proposes a genetic linkage between *CmFLS2* and a gene responsible for some advantageous trait. For instance, a recent study (Oren et al., 2022) mapped a major QTL for early flowering on melon chromosome 8, with the candidate gene (MELO3C007661) located approximately 3.3 Mb from *CmFLS2* in the DHL92 genome

(v3.6.1). Linkage dragging by such a gene could unexpectedly contribute to the predominance of *CmFLS2* haplotype II in improved *melo* accessions.

The second hypothesis is that carrying the functional *CmFLS2* haplotype I may no longer confer strong advantages in modern melon cultivation practices, which mostly take place under intensively controlled environments. In that situation, *FLS2*-dependent recognition of bacteria including non-adapted species might have a negative impact on the growth of melon by wasting energy unnecessarily. We also found that the *CmFLS2* haplotype I is highly conserved in tropical regions of Central America, Africa, and Southeast Asia (Figure S12). Given the higher abundance of plant pathogenic bacteria in tropical regions compared to other regions (Jones & Barbetti, 2012; Mansfield et al., 2012), the distribution of *CmFLS2* haplotypes may also be linked to regional variability in the risk of bacterial diseases. In any case, further studies, including genetic analyses of the relevant genes and cultivation tests under different environmental conditions, will be needed to test these hypotheses and unravel this intriguing puzzle.

In conclusion, our work strongly suggests that human domestication has led to the loss of a gene involved in plant immunity against bacterial pathogens. To date, a limited number of disease resistance genes have been identified in a few melon accessions. Resistance gene markers have been developed for genes that confer melon resistance against Fusarium wilt disease, cucumber mosaic virus, and powdery mildew (Guiu-Aragonés et al., 2014; Joobeur et al., 2004; Li et al., 2017; Tezuka et al., 2009). Little attention has been paid to developing molecular markers for melon bacterial resistance genes. Our study has demonstrated that *CmFLS2* genotypes can be easily investigated across the diverse germplasm panel using the PCR markers that are based on gene length differences. Melon breeders will benefit from this information for germplasm selection and preventing the potential loss of functional *CmFLS2*.

## EXPERIMENTAL PROCEDURES

### Plant materials and growth condition

Cucumber and melon seeds were sown in mixed culture soil (vermiculite: peat moss: Kon-pal = 1: 1: 1) and cultured in a growth chamber or greenhouse at 25°C with a photoperiod of 16 h.

### Synthetic peptides

The synthetic peptides we used were as follows: flg22, QRLSTGSRINSKDDAAGLQIA; flg22<sup>Pst</sup>, TRLSGLKINSKDDAAGMQIA. Each peptide was dissolved in sterile distilled water.

### Measurement of ROS

A luminol-based assay was employed to monitor the production of ROS (Keppler et al., 1989). Leaf discs (diameter, 5 mm) were cut from true leaves of each cucurbit plant using a cork borer and

were incubated with distilled water in the dark overnight and were then placed in a 96-well plate with 50  $\mu$ l of distilled water. Twelve individual leaf discs were taken from a single plant. To measure ROS production triggered by flg22, leaf discs were treated with 50  $\mu$ l of assay solution containing 400  $\mu$ M luminol (Sigma–Aldrich; A8511-5G), 20  $\mu$ g/ml horseradish peroxidase (Sigma–Aldrich; P6782), and either 1  $\mu$ M flg22 (Invitrogen) or 1  $\mu$ M flg22<sup>PSI</sup> (Eurofins). For measuring ROS production triggered by chitin, leaf discs were treated with 50  $\mu$ l of assay solution containing 400  $\mu$ M L-012 (FUJIFILM Wako Chemicals; 120-04891), 20  $\mu$ g/ml horseradish peroxidase, and 400  $\mu$ g/ml chitin (Sigma–Aldrich; C9752). Luminescence was detected as relative light units (RLUs) for 60 min using a Luminoskan Ascent 2.1 (Thermo Fisher Scientific).

### Plasmid construction

The sequences of *CsPDS*, *CmPDS*, *CsFLS2*, and *CmFLS2 I* fragments (300 bp) used for gene silencing were amplified from the cDNA of cucumber (cv. Suoyo) and melon (cv. Lennon) using gene-specific primer pairs (Table S4). The DNA products and the empty vector pBICAL2 were double-digested with *XhoI* and *BamHI*. The cut fragments were then ligated with digested pBICAL2 using a DNA Ligation Kit (Takara). The resultant constructs were designated as ALSV-*CsPDS*, ALSV-*CmPDS*, ALSV-*CsFLS2*, and ALSV-*CmFLS2-I*.

### ALSV-mediated VIGS

Each constructed plasmid and the empty vector pBICAL1 were transformed into *Agrobacterium tumefaciens* GV3101 (pMP90) by electroporation (Koncz & Schell, 1986). The transformed *Agrobacterium* was pre-cultured for 2 days at 28°C in dark conditions and then incubated overnight with shaking in liquid YEP medium containing kanamycin (50  $\mu$ g/ml), rifampicin (50  $\mu$ g/ml), and gentamicin (50  $\mu$ g/ml). The bacterial cultures were centrifuged at 3000 rpm at 4°C for 10 min and then suspended in washing buffer [10 mM MgCl<sub>2</sub>, 1 mM MES, 200  $\mu$ M acetosyringone (pH 5.6)]. After re-centrifuging at 3000 rpm at 4°C for 10 min, the bacterial pellet was resuspended in infiltration buffer [10 mM MgCl<sub>2</sub>, 200  $\mu$ M acetosyringone]. *Agrobacterium* containing pBICAL1 was mixed with each gene fragment-carrying strain in a 1:1 ratio in infiltration buffer, to a final OD<sub>600</sub> of 0.3. *Agrobacterium* preparations were infiltrated into 8-day-old melon and cucumber cotyledons from the abaxial surface using a needleless syringe.

### Quantitative RT-PCR and quantitative PCR

To detect *FLS2* gene expression in VIGS plants, cucumber or melon RNA was isolated from fourth true leaves (counting from bottom to top) using an RNeasy Plant Mini Kit (QIAGEN) and reverse transcribed using Takara Prime Script RT Master Mix (Takara Bio). The cDNA was then subjected to qPCR reactions using Takara TB Green Premix Ex Taq (Tli RNaseH Plus). The PCR reaction involved an initial denaturation at 95°C for 30 sec followed by 40 cycles of 95°C for 5 sec and 60°C for 30 sec, using a CFX Connect Real-Time PCR Detection System (Bio-Rad). Lennon- and Suoyo-specific primer pairs (Table S4) were used to detect *FLS2* expression. Relative gene expression was calculated by deducting the Ct value of an internal control gene from that of the target gene and represented as 2<sup>(-ΔCt)</sup>. Melon *Actin* (MU51303) and cucumber *Actin* (CsaV3\_2G018090) were used as the internal control in each reaction for normalization of gene expression level in RT-qPCR for Lennon and Suoyo, respectively. Quantitative PCR to evaluate *Psl* growth on plants used a DNA-based real-time PCR assay, as described previously (Ross & Somssich, 2016). Briefly, DNA for quantification of *Psl* growth on

melon was extracted using the DNeasy Plant Mini kit (QIAGEN) and then subjected to qPCR with the same conditions as described above. An *oprF* gene-specific primer pair (Table S4) was used to measure *Psl* biomass in plants. By subtracting the Ct value of the *oprF* gene from that of the melon *Actin* gene (ΔCT), the relative abundance of bacterial cells in relation to the quantity of plant cells was monitored.

### Statistics

Statistical significance was determined using a two-tailed *t*-test in each experiment and is represented by asterisks; \**P* < 0.05, \*\* < 0.01.

### Genome analysis of melon cv. Lennon

Genomic DNA of Lennon was extracted from fresh cotyledons using a DNeasy Plant Mini kit (QIAGEN) and sequenced on the Illumina NovaSeq 6000 platform, generating 150-bp paired-end reads. To search for the *FLS2* gene, the obtained sequence reads were mapped to the reference genome DHL92 (v 3.6.1) (Garcia-Mas et al., 2012) using BWA v0.7.17 (Li & Durbin, 2009) and SAMtools v1.15.1 (Li et al., 2009). IGV v2.7.2 (Robinson et al., 2017) was used to visualize and confirm the read mapping result.

### Genotyping of *FLS2* in cucurbits

Genomic DNA was extracted from the cotyledon of each cucurbit plant using the DNeasy Plant Mini kit (QIAGEN), and the bulk DNA of four individuals of each accession was used as the template for genome PCR. Genome PCR was performed using KOD One PCR Master Mix (TOYOBO) with the following program: 2 min at 94°C followed by 35 cycles of 10 sec at 98°C, 5 sec at 65°C, and 20 sec at 68°C. The primer pair CsCmFLS2\_check\_Fw/CsCmFLS2\_check\_Rv (Table S4) was used to amplify the *FLS2* locus in cucumber and melon. PCR products were loaded on 1% agarose gels.

### *P. syringae* pv. *lachrymans* (*Psl*) infection assay on melon

The *Psl* strain MAFF301315 (MAFF Genebank) was grown on NYGA medium (per liter: 5 g peptone, 3 g dried yeast extract, 20 ml glycerol, 1.5% agar) and pre-cultured for 3 days at 28°C in dark conditions. The strain was then incubated in 10 ml NYGA liquid medium for 16 h at 28°C with shaking. For inoculation of *Psl* on ALSV-EV and ALSV-*CmFLS2I* plants, the bacterial culture was centrifuged and resuspended in 1 mM MgCl<sub>2</sub> and adjusted to 4 × 10<sup>8</sup> cfu/ml. After adding 0.04% Silwet L-77 to the prepared bacterial suspension, about 2 ml per leaf was spray-inoculated onto the surface of the fourth true leaves (counting from bottom to top). The treated plants were put into a plastic box (six plants per box) under artificial lighting with 45% relative humidity at 24–25°C for 1 h. The box was then closed to maintain 100% relative humidity and kept under the long-day condition with 16 h illumination per day. After 72 h, the lid was opened, maintaining the plants under the same condition but with 45% relative humidity for 24 h. Inoculation results were observed at 4 days after inoculation. Forty-day-old Lennon VIGS plants were used for *Psl* spray inoculation. For inoculation of *Psl* on melon cultivars EDISTO 47 (INRA) and Harukei3, we used a lower concentration of *Psl* inoculum for spraying because the seedlings used for this experiment were younger than for *Psl* inoculation on gene-silenced plants. The bacterial culture was centrifuged and resuspended in 1 mM MgCl<sub>2</sub> and adjusted to 5 × 10<sup>7</sup> cfu/ml. After adding 0.01% Silwet L-77 to the prepared bacterial suspension, about 0.5 ml per leaf was spray-inoculated onto the upper surface of the first true leaves. The conditions for bacterial infection and observation were

the same as mentioned above. Twenty-day-old melon plants were used for *PstI* spray inoculation.

### Phylogenetic analysis

The accessions shown in Table S1 were used to construct a phylogenetic tree (Figure 6a). These accessions were selected to encompass the genetic diversity of each group of cytoplasm type (Tanaka et al., 2013). The phylogenetic tree was constructed as described previously (Shigita et al., 2023).

### Genotyping of *CmFLS2* using SRA data

We used Sequence Reads Archive (SRA) data randomly selected to cover at least 10% of the accessions from each group shown in Liu et al. (2020) and Zhao et al. (2019) (Table S3). BWA v0.7.17 was used for mapping the SRA data to *CmFLS2* haplotypes I and II. The resulting alignments were subsequently assessed for coverage using SAMtools v1.15.1. By examining the coverage of each haplotype, we assessed the presence or absence of each haplotype in corresponding accessions (if the breadth coverage reached 90% or higher, it was regarded as the presence of that haplotype).

### AUTHOR CONTRIBUTIONS

CJ and YT designed research; CJ, HM, and YN performed research; CJ, HM, YI, and GS analyzed the data; CJ, HM, GS, KK, and YT wrote the paper.

### ACKNOWLEDGMENTS

We thank the MAFF Genebank for providing the *PstI* strain MAFF301315. We also thank M. Kaido and N. Yoshikawa for providing ALSV vectors. We also thank K. Yoshida for technical advice and sharing the field. We are grateful to J. Shimazu, R. Tsujita, and Y. Yoshioka for providing plant materials. This work was supported by Grants-in-Aid for Scientific Research (21H05032 to YT and 23KJ1148 to HM) (KAKENHI) and JST SPRING, Grant Number JPMJSP2110 (to CJ).

### CONFLICT OF INTEREST

The authors declare no conflict of interest.

### DATA AVAILABILITY STATEMENT

The data that support the findings of this study are available in the Supporting Information of this article. Nucleotide sequence data reported herein are available in the DNA Data Bank of Japan (DDBJ) Sequence Read Archive under accession number DRA017694.

### SUPPORTING INFORMATION

Additional Supporting Information may be found in the online version of this article.

**Figure S1.** Amino acid sequence alignment of CsFLS2 with its orthologs in other plants.

**Figure S2.** Deduced amino acid sequence of CsFLS2.

**Figure S3.** Virus-induced gene silencing of *PDS* gene in cucurbit plants.

**Figure S4.** Plant growth of *FLS2*-silenced cucumber plants.

**Figure S5.** Deduced amino acid sequence of *CmFLS2*.

**Figure S6.** Amino acid sequence alignment of FLS2 haplotypes in melon (Lennon) with FLS2 in cucumber.

**Figure S7.** Alignment of re-sequencing reads of Suvo with the *CsFLS2* region of four cucumber reference genomes.

**Figure S8.** Genotyping of *FLS2* locus in progeny of *FLS2* homozygous cucumber and melon accessions.

**Figure S9.** Chitin- or flg22-triggered ROS assay in melon cultivars lacking functional *CmFLS2* and in Lennon.

**Figure S10.** Proportion of each *CmFLS2* haplotype in different commercial F<sub>1</sub> hybrid cultivars.

**Figure S11.** Amino acid sequence alignment of cucumber FLS2 with its homologues in other cucurbit plants.

**Figure S12.** Geographic distribution of two haplotypes of *CmFLS2*.

**Table S1.** Summary of the sampled collection of cucurbit accessions.

**Table S2.** Summary of the sampled collection of commercial cultivars.

**Table S3.** Summary of the sampled collection of SRA data.

**Table S4.** Primer list for gene amplification and qPCR analysis.

### REFERENCES

- Akköprü, A., Akat, Ş., Özaktan, H., Gül, A. & Akbaba, M. (2021) The long-term colonization dynamics of endophytic bacteria in cucumber plants, and their effects on yield, fruit quality and angular leaf spot disease. *Scientia Horticulturae*, **282**, 110005.
- Boutrot, F. & Zipfel, C. (2017) Function, discovery, and exploitation of plant pattern recognition receptors for broad-spectrum disease resistance. *Annual Review of Phytopathology*, **55**, 257–286.
- Burdman, S. & Walcott, R.O.N. (2012) *Acidovorax citrulli*: generating basic and applied knowledge to tackle a global threat to the cucurbit industry. *Molecular Plant Pathology*, **13**, 805–815.
- Chai, A., Yuan, L., Li, L., Shi, Y., Xie, X., Wang, Q. et al. (2020) Aerosol transmission of *Pseudomonas amygdali* pv. *lachrymans* in greenhouses. *Science of the Total Environment*, **748**, 141433.
- Cheng, Q., Xiao, H. & Xiong, Q. (2020) Conserved exons of FLAGELLIN-SENSING 2 (FLS2) across dicot plants and their functions. *Plant Science*, **296**, 110507.
- Chinchilla, D., Bauer, Z., Regenass, M., Boller, T. & Felix, G. (2006) The Arabidopsis receptor kinase FLS2 binds flg22 and determines the specificity of flagellin perception. *Plant Cell*, **18**, 465–476.
- Couto, D. & Zipfel, C. (2016) Regulation of pattern recognition receptor signalling in plants. *Nature Reviews Immunology*, **16**, 537–552.
- Endl, J., Achigan-Dako, E.G., Pandey, A.K., Monforte, A.J., Pico, B. & Schaefer, H. (2018) Repeated domestication of melon (*Cucumis melo*) in Africa and Asia and a new close relative from India. *American Journal of Botany*, **105**, 1662–1671.
- Felix, G., Duran, J.D., Volko, S. & Boller, T. (1999) Plants have a sensitive perception system for the most conserved domain of bacterial flagellin. *The Plant Journal*, **18**, 265–276.
- Finlay, B.B. & Falkow, S. (1997) Common themes in microbial pathogenicity revisited. *Microbiology and Molecular Biology Reviews*, **61**, 136–169.
- García-Mas, J., Benjak, A., Sanseverino, W., Bourgeois, M., Mir, G., González, V.M. et al. (2012) The genome of melon (*Cucumis melo* L.). *Proceedings of the National Academy of Sciences of the United States of America*, **109**, 11872–11877.
- Gómez-Gómez, L. & Boller, T. (2000) FLS2: an LRR receptor-like kinase involved in the perception of the bacterial elicitor flagellin in Arabidopsis. *Molecular Cell*, **5**, 1003–1011.
- Gómez-Gómez, L. & Boller, T. (2002) Flagellin perception: a paradigm for innate immunity. *Trends in Plant Science*, **7**, 251–256.
- Guiu-Aragonés, C., Monforte, A.J., Saladié, M., Correa, R.X., García-Mas, J. & Martín-Hernández, A.M. (2014) The complex resistance to cucumber mosaic cucumovirus (CMV) in the melon accession PI161375 is governed by one gene and at least two quantitative trait loci. *Molecular Breeding*, **34**, 351–362.
- Hann, D.R. & Rathjen, J.P. (2007) Early events in the pathogenicity of *Pseudomonas syringae* on *Nicotiana benthamiana*. *The Plant Journal*, **49**, 607–618.

- Igarashi, A., Yamagata, K., Sugai, T., Takahashi, Y., Sugawara, E., Tamura, A. *et al.* (2009) Apple latent spherical virus vectors for reliable and effective virus-induced gene silencing among a broad range of plants including tobacco, tomato, *Arabidopsis thaliana*, cucurbits, and legumes. *Virology*, **386**, 407–416.
- Jones, R.A. & Barbetti, M.J. (2012) Influence of climate change on plant disease infections and epidemics caused by viruses and bacteria. *CABI Reviews*, **7**, 1–31.
- Joobeur, T., King, J.J., Nolin, S.J., Thomas, C.E. & Dean, R.A. (2004) The fusarium wilt resistance locus Fom-2 of melon contains a single resistance gene with complex features. *The Plant Journal*, **39**, 283–297.
- Kawai, T., Gono, A., Nitta, M., Kaido, M., Yamagishi, N., Yoshikawa, N. *et al.* (2014) Virus-induced gene silencing in apricot (*Prunus armeniaca* L.) and Japanese apricot (*P. mume* Siebold & Zucc.) with the apple latent spherical virus vector system. *Journal of the Japanese Society for Horticultural Science*, **83**, 23–31.
- Keppeler, L.D., Baker, C.J. & Atkinson, M.M. (1989) Active oxygen production during a bacteria-induced hypersensitive reaction in tobacco suspension cells. *Phytopathology*, **79**, 974–978.
- Khlaif, H. (1995) Varietal reaction and control of angular leaf spot disease on cucumber. *Pure and Applied Science*, **22**, 1201–1208.
- Kirkbride, J.H. (1993) *Biosystematic Monograph of the Genus Cucumis (Cucurbitaceae): Botanical Identification of Cucumbers and Melons*. Boone, NC: Parkway Publishers.
- Koncz, C. & Schell, J. (1986) The promoter of T<sub>1</sub>-DNA gene 5 controls the tissue-specific expression of chimaeric genes carried by a novel type of *agrobacterium* binary vector. *Molecular and General Genetics*, **204**, 383–396.
- Li, B., Zhao, Y., Zhu, Q., Zhang, Z., Fan, C., Amanullah, S. *et al.* (2017) Mapping of powdery mildew resistance genes in melon (*Cucumis melo* L.) by bulked segregant analysis. *Scientia Horticulturae*, **220**, 160–167.
- Li, H. & Durbin, R. (2009) Fast and accurate short read alignment with burrows-wheeler transform. *Bioinformatics*, **25**, 1754–1760.
- Li, H., Handsaker, B., Wysoker, A., Fennell, T., Ruan, J., Homer, N. *et al.* (2009) The sequence alignment/map format and SAMtools. *Bioinformatics*, **25**, 2078–2079.
- Liu, S., Gao, P., Zhu, Q., Zhu, Z., Liu, H., Wang, X. *et al.* (2020) Resequencing of 297 melon accessions reveals the genomic history of improvement and loci related to fruit traits in melon. *Plant Biotechnology Journal*, **18**, 2545–2558.
- Macho, A.P. & Zipfel, C. (2014) Plant PRRs and the activation of innate immune signaling. *Molecular Cell*, **54**, 263–272.
- Mansfield, J., Genin, S., Magori, S., Citovsky, V., Sriariyanum, M., Ronald, P. *et al.* (2012) Top 10 plant pathogenic bacteria in molecular plant pathology. *Molecular Plant Pathology*, **13**, 614–629.
- Monaghan, J. & Zipfel, C. (2012) Plant pattern recognition receptor complexes at the plasma membrane. *Current Opinion in Plant Biology*, **15**, 349–357.
- Newberry, E.A., Jardini, T.M., Rubio, I., Roberts, P.D., Babu, B., Koike, S.T. *et al.* (2016) Angular leaf spot of cucurbits is associated with genetically diverse *pseudomonas syringae* strains. *Plant Disease*, **100**, 1397–1404.
- Ogunbanjo, O., Onawumi, O., Gbadamosi, M., Ogunlana, A. & Anselm, O. (2016) Chemical speciation of some heavy metals and human health risk assessment in soil around two municipal dumpsites in Sagamu, Ogun state, Nigeria. *Chemical Speciation and Bioavailability*, **28**, 142–151.
- Olczak-Woltman, H., Masny, A., Bartoszewski, G., Płucienniczak, A. & Niemirowicz-Szczytt, K. (2006) Genetic diversity of *Pseudomonas syringae* pv. *lachrymans* strains isolated from cucumber leaves collected in Poland. *Plant Pathology*, **56**, 373–382.
- Olczak-Woltman, H., Schollenberger, M., Mądry, W. & Niemirowicz-Szczytt, K. (2008) Evaluation of cucumber (*Cucumis sativus*) cultivars grown in Eastern Europe and progress in breeding for resistance to angular leaf spot (*Pseudomonas syringae* pv. *lachrymans*). *European Journal of Plant Pathology*, **122**, 385–393.
- Oren, E., Tzuri, G., Dafna, A., Rees, E.R., Song, B., Freilich, S. *et al.* (2022) QTL mapping and genomic analyses of earliness and fruit ripening traits in a melon recombinant inbred lines population supported by de novo assembly of their parental genomes. *Horticulture Research*, **9**, uhab081.
- Pohronezny, K., Larsen, P.O. & Leben, C. (1978) Observations on cucumber fruit invasion by *Pseudomonas lachrymans*. *Plant Disease Report*, **62**, 306–309.
- Renner, S.S. & Schaefer, H. (2016) Phylogeny and evolution of the Cucurbitaceae genetics and genomics of Cucurbitaceae. In: Grumet, R., Katzir, N. & Garcia-Mas, J. (Eds.) *Genetics and Genomics of Cucurbitaceae*. Switzerland: Springer International, pp. 13–23.
- Robatzek, S., Bittel, P., Chinchilla, D., Köchner, P., Felix, G., Shiu, S.H. *et al.* (2007) Molecular identification and characterization of the tomato flagellin receptor LeFLS2, an orthologue of Arabidopsis FLS2 exhibiting characteristically different perception specificities. *Plant Molecular Biology*, **64**, 539–547.
- Roberts, R., Liu, A.E., Wan, L., Geiger, A.M., Hind, S.R., Rosli, H.G. *et al.* (2020) Molecular characterization of differences between the tomato immune receptors Flagellin sensing 3 and Flagellin sensing 2. *Plant Physiology*, **183**, 1825–1837.
- Robinson, J.T., Thorvaldsdóttir, H., Wenger, A.M., Zehir, A. & Mesirov, J.P. (2017) Variant review with the integrative genomics viewer. *Cancer Research*, **77**, e31–e34.
- Rolnik, A. & Olas, B. (2020) Vegetables from the Cucurbitaceae family and their products: positive effect on human health. *Nutrition*, **78**, 110788.
- Ross, A. & Somssich, I.E. (2016) A DNA-based real-time PCR assay for robust growth quantification of the bacterial pathogen *pseudomonas syringae* on *Arabidopsis thaliana*. *Plant Methods*, **12**, 1–8.
- Saijo, Y., Loo, E.P.I. & Yasuda, S. (2018) Pattern recognition receptors and signaling in plant-microbe interactions. *The Plant Journal*, **93**, 592–613.
- Sanseverino, W., Hénaff, E., Vives, C., Pinosio, S., Burgos-Paz, W., Morgante, M. *et al.* (2015) Transposon insertions, structural variations, and SNPs contribute to the evolution of the melon genome. *Molecular Biology and Evolution*, **32**, 2760–2774.
- Shi, Q., Febres, V.J., Jones, J.B. & Moore, G.A. (2016) A survey of *FLS2* genes from multiple citrus species identifies candidates for enhancing disease resistance to *Xanthomonas citri* ssp. *citri*. *Horticulture Research*, **3**, 16022.
- Shigita, G., Dung, T.P., Pervin, M.N., Duong, T.T., Imoh, O.N., Monden, Y. *et al.* (2023) Elucidation of genetic variation and population structure of melon genetic resources in the NARO Genebank, and construction of the world melon Core collection. *Breeding Science*, **73**, 269–277.
- Takai, R., Isogai, A., Takayama, S. & Che, F.S. (2008) Analysis of flagellin perception mediated by flg22 receptor OsFLS2 in rice. *Molecular Plant-Microbe Interactions*, **21**, 1635–1642.
- Tanaka, K., Akashi, Y., Fukunaga, K., Yamamoto, T., Aierken, Y., Nishida, H. *et al.* (2013) Diversification and genetic differentiation of cultivated melon inferred from sequence polymorphism in the chloroplast genome. *Breeding Science*, **63**, 183–196.
- Tans-Kersten, J., Huang, H. & Allen, C. (2001) *Ralstonia solanacearum* needs motility for invasive virulence on tomato. *Journal of Bacteriology*, **183**, 3597–3605.
- Tezuka, T., Waki, K., Yashiro, K., Kuzuya, M., Ishikawa, T., Takatsu, Y. *et al.* (2009) Construction of a linkage map and identification of DNA markers linked to *Fom-1*, a gene conferring resistance to *Fusarium oxysporum* f. sp. *melonis* race 2 in melon. *Euphytica*, **168**, 177–188.
- Tian, S.N., Liu, D.D., Zhong, C.L., Xu, H.Y., Yang, S., Fang, Y. *et al.* (2020) Silencing *GmFLS2* enhances the susceptibility of soybean to bacterial pathogen through attenuating the activation of GmMAPK signaling pathway. *Plant Science*, **292**, 110386.
- Trdá, L., Fernandez, O., Boutrot, F., Héloir, M.C., Kelloniemi, J., Daire, X. *et al.* (2014) The grapevine flagellin receptor VvFLS2 differentially recognizes flagellin-derived epitopes from the endophytic growth-promoting bacterium *Burkholderia phytofirmans* and plant pathogenic bacteria. *New Phytologist*, **201**, 1371–1384.
- Wu, L., Xiao, H., Zhao, L. & Cheng, Q. (2022) CRISPR/Cas9-mediated generation of *fls2* mutant in *Nicotiana benthamiana* for investigating the flagellin recognition spectrum of diverse FLS2 receptors. *Plant Biotechnology Journal*, **20**, 1853–1855.
- Yuan, M., Ngou, B.P.M., Ding, P. & Xin, X.F. (2021) PTI-ETI crosstalk: an integrative view of plant immunity. *Current Opinion in Plant Biology*, **62**, 102030.
- Zhao, G., Lian, Q., Zhang, Z., Fu, Q., He, Y., Ma, S. *et al.* (2019) A comprehensive genome variation map of melon identifies multiple domestication events and loci influencing agronomic traits. *Nature Genetics*, **51**, 1607–1615.
- Zipfel, C., Robatzek, S., Navarro, L., Oakeley, E.J., Jones, J.D., Felix, G. *et al.* (2004) Bacterial disease resistance in Arabidopsis through flagellin perception. *Nature*, **428**, 764–767.